

Supporting Information

Non-Interpenetrated Cu-based MOF Constructed from a Rediscovered Tetrahedral Ligand**

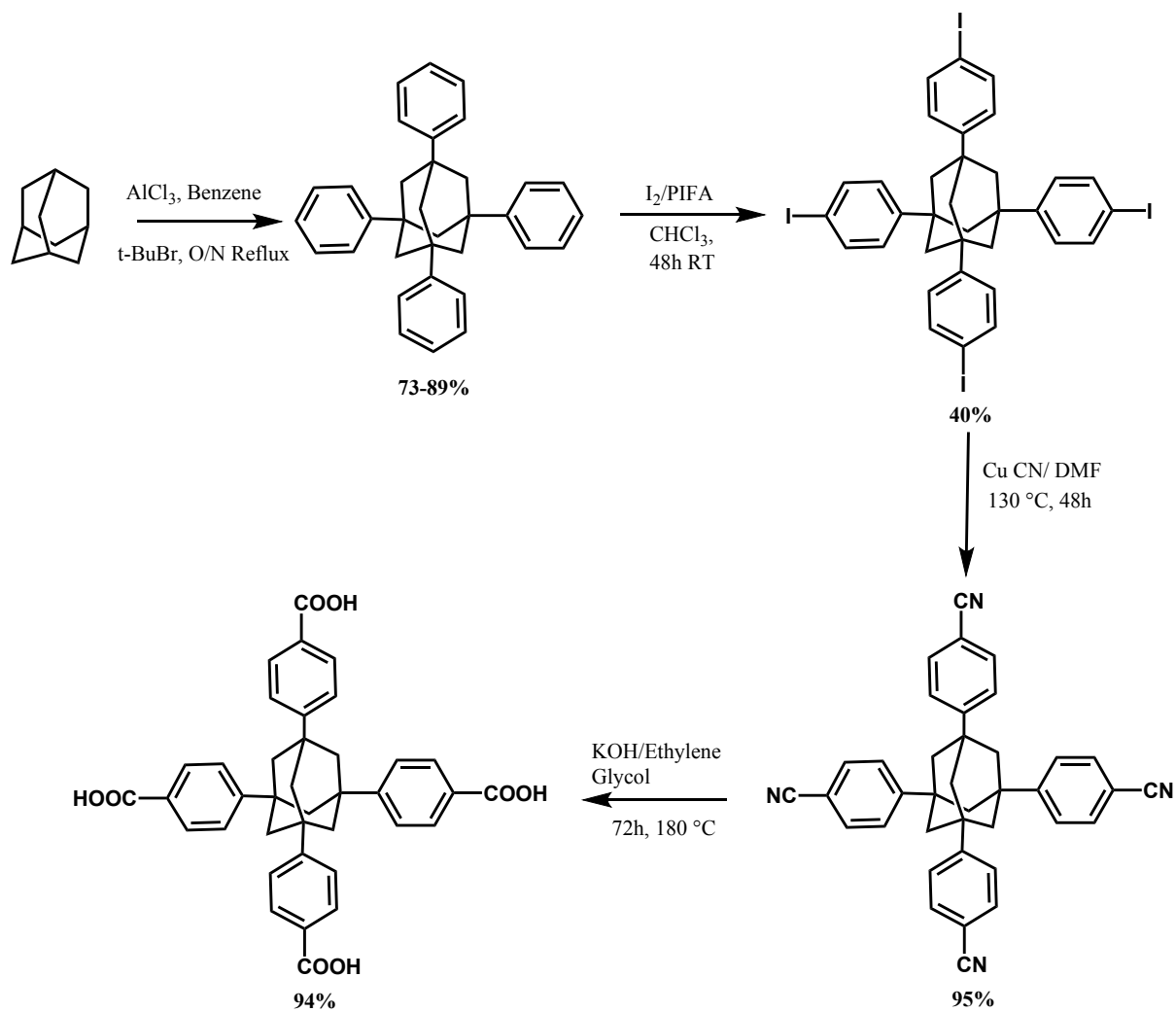
Komal M. Patil,^a Shane G. Telfer,^b Stephen C. Moratti,^a Omid T. Qazvini^b and Lyall R. Hanton^{a,*}

- a. Department of Chemistry, *Te Tari Hua-Ruanuku*, University of Otago, P. O. Box 56, Dunedin 9054, New Zealand.
- b. MacDiarmid Institute of Advanced Materials and Nanotechnology, Institute of Fundamental Sciences, Massey University, Palmerston North 4474, New Zealand.

Table of Contents

| | |
|--|-----------|
| SUPPORTING INFORMATION | S1 |
| S1.1 SYNTHESIS OF LIGAND (L) | S2 |
| S1.2 SYNTHESIS AND X-RAY STRUCTURE SOLUTION DETAILS FOR UOF-1 | S3 |
| S1.3 SELECTED DETAILS OF DATA COLLECTIONS AND STRUCTURE REFINEMENTS | S6 |
| S1.4 THERMAL ANALYSIS (TGA AND DSC) | S7 |
| S1.5 POWDER X-RAY ANALYSIS | S9 |
| S1.6 ACTIVATION TECHNIQUES | S10 |
| S1.7 GAS ADSORPTION ISOTHERMS OF UOF-1 | S12 |
| S1.8 COMPARATIVE DATA OF CU-PTS STRUCTURES IN THE LITERATURE | S17 |
| S1.9 IDEAL ADSORBED SOLUTION THEORY (IAST) CALCULATIONS | S18 |
| S1.10 HEAT OF ADSORPTION (Q_{st}) CALCULATIONS | S20 |
| S1.11 REFERENCES | S23 |

S1.1 Synthesis of Ligand (L)



Scheme S1. Synthesis of 1,3,5,7-tetrakis(4-carboxyphenyl)adamantane (**L**).

S1.2 Synthesis and X-ray structure solution details for UOF-1

The solvothermal reaction of $\text{Cu}(\text{NO}_3)_2 \cdot 3\text{H}_2\text{O}$ and **L** in 1:1 v/v solvent mixture of DMF and $\text{C}_2\text{H}_5\text{OH}$ was carried out in a pressure tube. The pressure tube was protected with a thick steel blast tube and subjected to a heating regime of slowly raising the temperature to 120 °C over six hours, maintaining the temperature at 120 °C for 48 hours and then slowly cooling to room temperature at about 2 °C/hour. This heating regime resulted in a brown precipitate. The precipitate was dissolved with 4 drops of conc. HCl and further heated for seven days at 170 °C and again cooled to room temperature at about 2 °C/hour to produce a blue solution. To an aliquot of this solution, CH_2Cl_2 was slowly diffused in for about two months and resulted in the formation of turquoise crystals of **UOF-1.DMF** (procedure 1) in very small quantities (Figure S1).

Two data sets were collected on this compound, however, the quality of the data was very poor. Many attempts to reproduce these crystals, by varying the solvents and Cu(II) salts and using acids such as HCl and HNO_3 at various stages of synthesis, and also by varying reaction conditions, were unsuccessful. In most of the cases, either clear solutions or very small quantities of microcrystalline precipitates were obtained. In an attempt to improve the quantity and quality of the crystals, the following modifications were successful. Concentrated HCl was replaced by dilute HBF_4 (2.4% v/v dilution in DMF) and instead of using pressure tubes and a heating and cooling regime, the reaction was carried in a Borosil vial by heating the reaction mixture in an isothermal oven at 80 °C for about 24 hours. The resultant crystals, of **UOF-1.DMF** (procedure 2, Figure S1), obtained by adopting these modifications were in better yield and were also straightforward to synthesise when compared to the previous method. The quality of the single crystals was also poor and the crystals did not diffract beyond a resolution of 1.75 Å. Importantly, the cell dimensions for crystals of both the **UOF-1.DMF** samples were the same indicating an efficient synthesis of this MOF with time of synthesis reduced from 2-3 months to 24 hours. Infrared analysis of a crystalline sample of **UOF-1.DMF** confirmed the presence of **L** as the peaks at 2926–2853 (adamantyl C–H group), 1702 (C–O stretching), 1607 and 1544 (C=C bending, COO^- asymmetric stretching), 1401 (COO^- symmetric stretching) and 763–526 cm^{-1} (aromatic C–H bending) were observed. The IR spectrum indicated complete deprotonation of the **L** ligand as the O–H stretches and bends in the regions of 1289–1271 and 1083–1042 cm^{-1} were very weak. These peaks were very strong in the IR spectrum of the native **L** ligand. The $\Delta\nu$

value, i.e. the difference between the $\nu_{\text{asym}}(\text{COO})$ and $\nu_{\text{sym}}(\text{COO})$, between 143–206 cm^{-1} indicated that the carboxylate groups were bound to the Cu(II) cations in a symmetric bridging mode.^{1, 2} There were problems in obtaining consistent microanalysis for these materials. To address this issue, several crystals were manually separated from a number of crystal jars, washed with acetone, dried *in vacuo* and microanalysed. It was found that for three such analyses the C, H and N values ranged between 50.5–52.3%, 4.2–4.6% and 1.4–3.8%, respectively. The calculated C, H and N values for the completely desolvated framework were 61.7%, 3.8% and 0.0% (Calc. for $\text{C}_{38}\text{H}_{28}\text{O}_8\text{Cu}_2$), respectively, and for the solvated framework as indicated by SCXRD these values were 53.4%, 7.3% and 10.9% (Calc. for $\text{C}_{38}\text{H}_{28}\text{O}_8\text{Cu}_2 \cdot 14\text{DMF} \cdot 2\text{H}_2\text{O}$), respectively. The traces of nitrogen in these samples could be due to residual DMF molecules. The lower carbon content than the completely desolvated framework suggested that the void space in the MOF might have been replaced by H_2O molecules from the atmosphere.

Three data sets were collected of this compound. The overall quality of data was poor, mainly because of the presence of a large number of uncoordinated and disordered solvent molecules within the structure. The solvent molecules in the structure were estimated using the PLATON SQUEEZE³ routine. In a total void volume of 4486 \AA^3 , 1905 electrons were SQUEEZEd from the structure. This residual electron density was assigned to 7 DMF molecules per Cu(II) cation.

[1905/4 = 291.25 e per Cu(II) cation ; 7(DMF) = 7(40) e = 280 e]

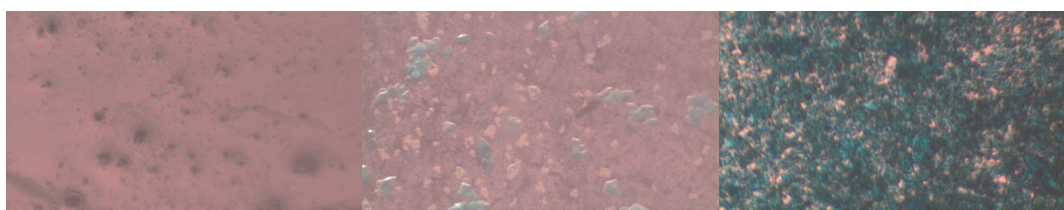


Figure S1. An image of the single crystals of **UOF-1.DMF** obtained from procedure **1** (left), procedure **2** (centre) and bulk synthesis of **UOF-1.DMF** (right) displaying the improvement in quality and quantity of crystals. The scale of these images is 100 μm .

In attempts to obtain better structure solution the DMF from the as-synthesized crystals was exchanged with acetone to yield turquoise coloured crystals of $\{[\text{Cu}_2(\text{L})(\text{H}_2\text{O})_2] \cdot 18(\text{CH}_3)_2\text{CO}\}_\infty$ (**UOF-1.(CH₃)₂CO**). The solvent molecules in the structure were estimated using the PLATON SQUEEZE³ routine. In a total void volume of 4447 \AA^3 , 1117 electrons

were SQUEEZEd from the structure. This residual electron density was assigned to 9 acetone molecules per Cu(II) cation.

$$[1117/4 = 279.25 \text{ e per Cu(II) cation ; } 9(\text{acetone}) = 9(32) \text{ e} = 288 \text{ e}]$$

After soaking the crystals in dry acetone, the solvent was removed and fresh DEF was added to yield turquoise coloured crystals of $\{[\text{Cu}_2(\text{L})(\text{H}_2\text{O})_2] \cdot 8\text{DEF}\}_\infty$ (**UOF-1.DEF**) and this structure was reported. The structure was severely disordered and contained large ADPs. Owing to the low data quality and that the solvent molecules were severely disordered, they could not be adequately located in the Fourier maps. The solvent molecules were SQUEEZEd from the structure using the PLATON SQUEEZE³ routine. SQUEEZing the structure resulted in significant reduction of the R_1 and wR_2 values. The R_1 and wR_2 values before SQUEEZing were 27.36% and 59.65%, respectively, while after SQUEEZing these values reduced to 9.67% and 30.27%, respectively. In a total void volume of 4349 Å³, 835 electrons were SQUEEZEd from the structure. This residual electron density was assigned to 4 DEF molecules per Cu(II) cation.

$$[835/4 = 208.75 \text{ e per Cu(II) cation ; } 4(\text{DEF}) = 4(56) \text{ e} = 224 \text{ e}]$$

The DMF from the as-synthesized crystals was exchanged with dry CH₂Cl₂ to yield dark blue coloured crystals. These dark blue crystals quickly changed its colour to green upon exposure to air. A dramatic change in space group from tetragonal $P4_2/mmc$ to a lower symmetry orthorhombic $Cccm$ (**UOF-1.CH₂Cl₂**) was observed. However, this change in space group had no impact on the **PtS** topology. The solvent molecules in the structure were estimated using the PLATON SQUEEZE³ routine. In a total void volume of 8791 Å³, 2468 electrons were SQUEEZEd from the structure. This residual electron density was assigned to 7 CH₂Cl₂ molecules per Cu(II) cation.

$$[2468/8 = 308.5 \text{ e per Cu(II) cation ; } 7(\text{CH}_2\text{Cl}_2) = 7(42) \text{ e} = 294 \text{ e}]$$

S1.3 Selected details of data collections and structure refinements

Table S1. Crystal data for UOF-1

| Structure | UOF-1.DMF (Procedure 1) | UOF-1.DMF (Procedure 2) | UOF-1.(CH ₃) ₂ CO | UOF-1.DEF | UOF-1.CH ₂ Cl ₂ |
|---|--|----------------------------|---|---|--|
| Formula | C ₁₉ H ₁₅ CuO ₅ (C ₃ H ₇ NO) ₇ | – | C ₁₉ H ₁₅ CuO ₅ (C ₃ H ₆ O) ₉ | C ₁₉ H ₁₅ CuO ₅ (C ₃ H ₁₁ NO) ₄ | C ₁₉ H ₁₅ CuO ₅ (CH ₂ Cl ₂) ₇ |
| Formula weight | 898.52 | – | 909.58 | 791.46 | 981.40 |
| Crystal System | Tetragonal | Tetragonal | Tetragonal | Tetragonal | Orthorhombic |
| Space group | <i>P4₂/mmc</i> | <i>P4₂/mmc</i> | <i>P4₂/mmc</i> | <i>P4₂/mmc</i> | <i>Cccm</i> |
| <i>a</i> /Å | 14.686(5) | 14.456(4) | 14.7093(16) | 14.3700(13) | 19.302(5) |
| <i>b</i> /Å | 14.686(5) | 14.456(4) | 14.7093(16) | 14.3700(13) | 21.805(4) |
| <i>c</i> /Å | 26.103(9) | 26.369(2) | 26.053(3) | 26.464(3) | 26.364(4) |
| α /° | 90 | 90 | 90 | 90 | 90 |
| β /° | 90 | 90 | 90 | 90 | 90 |
| γ /° | 90 | 90 | 90 | 90 | 90 |
| <i>V</i> /Å ³ | 5630(3) | 5511(2) | 5636.9(14) | 5464.8(12) | 11096(4) |
| <i>Z</i> | 4 | – | 4 | 4 | 8 |
| <i>T</i> /K | 100.0(2) | 100.0(2) | 100.0(2) | 100(2) | 100(2) |
| μ /mm ⁻¹ | 0.992 | – | 0.987 | 0.860 | 6.972 |
| Total reflections | 22352 | 41185 | 11025 | 10870 | 9509 |
| Unique reflections (<i>R</i> _{int}) | 2826 (0.3546) | 3099 (0.2132) | 1764 (0.1590) | 1696 (0.0835) | 2655 (0.0551) |
| Resolution Range | 3.452-67.989 | 3.485-74.342 | 3.004-67.684 | 3.075-51.813 | 3.487-52.644 |
| <i>R</i> ₁ indices [<i>I</i> >2σ(<i>I</i>)] | 0.1617 | – | 0.1241 | 0.0967 | 0.1329 |
| $\omega R2$ (all data) | 0.5054 | – | 0.3808 | 0.3027 | 0.3615 |
| Goodness-of-fit | 1.007 | – | 1.244 | 1.017 | 0.857 |
| Radiation type | Cu K α | Cu K α | Cu K α | Cu K α | Cu K α |

S1.4 Thermal Analysis (TGA and DSC)

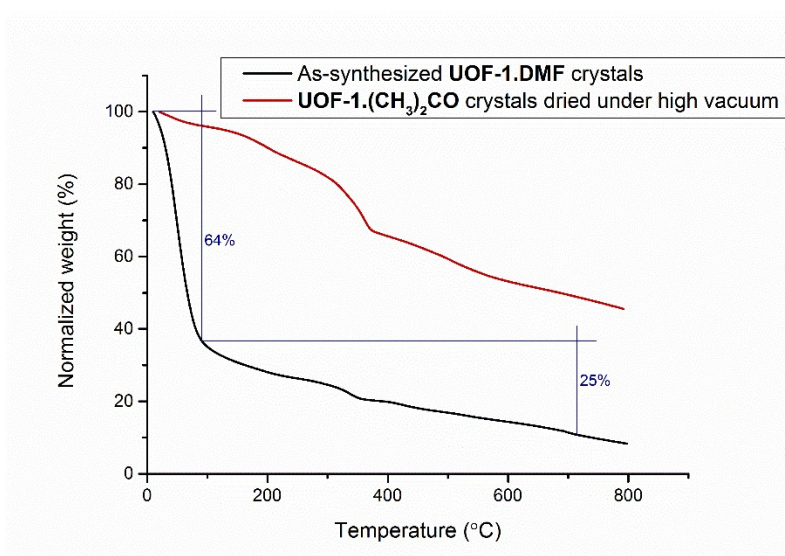


Figure S2. The thermograms showing concerted collapse of the framework after the initial loss of solvent molecules. These thermograms were obtained by heating the single crystals of **UOF-1.DMF** (in black) at a temperature increase rate of 5 °C/min and the vacuum dried crystals of **UOF-1.(CH₃)₂CO** (in red) at a temperature increase rate of 20 °C/min, both under a N₂ atmosphere.

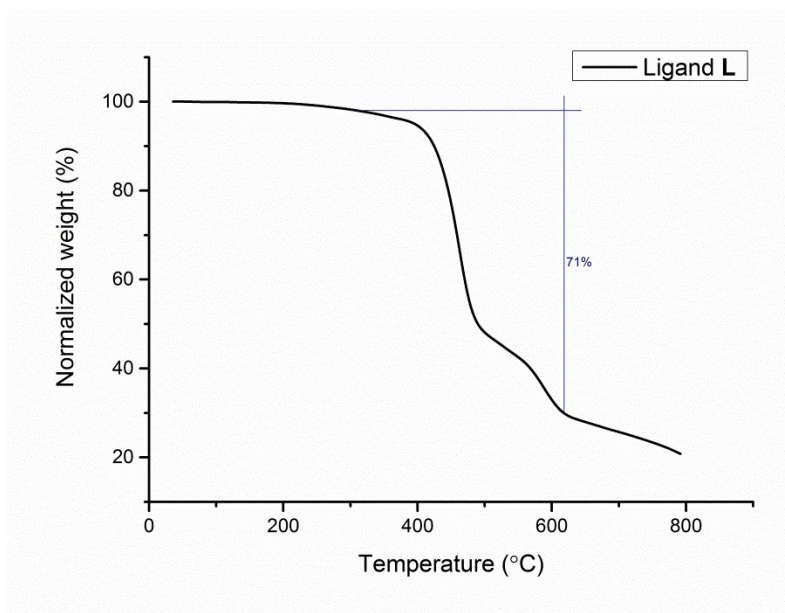


Figure S3 The thermogram of ligand **L** showing decomposition post 360 °C. This thermogram was obtained by heating native **L** at a temperature increase rate of 20 °C/min under a N₂ atmosphere.

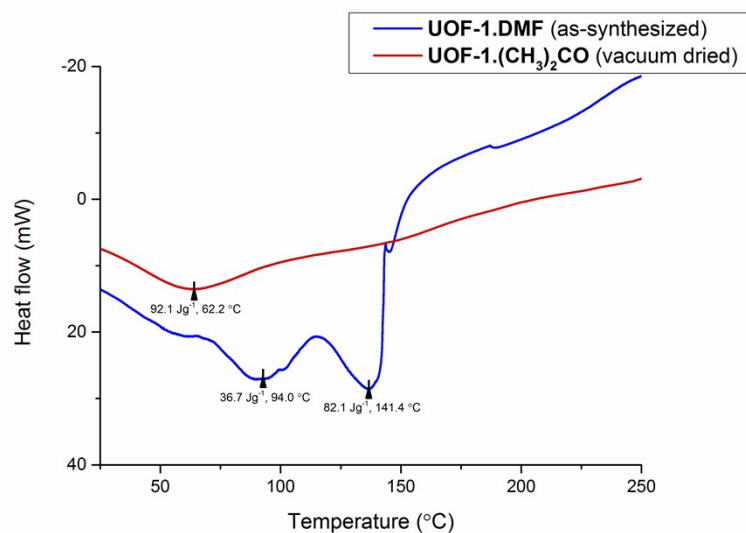


Figure S4. The DSC curves are obtained by heating the single crystals of as-synthesized **UOF-1.DMF** and vacuum dried **UOF-1.(CH₃)₂CO** at a temperature increase rate of 2 °C/min under a N₂ atmosphere. The DSC curve of **UOF-1.DMF** (in blue) shows the presence of H₂O and DMF in the crystals. The DSC curve of the vacuum dried **UOF-1.(CH₃)₂CO** (in red) shows the presence of acetone and some trace DMF in the crystals.

S1.5 Powder X-Ray Analysis

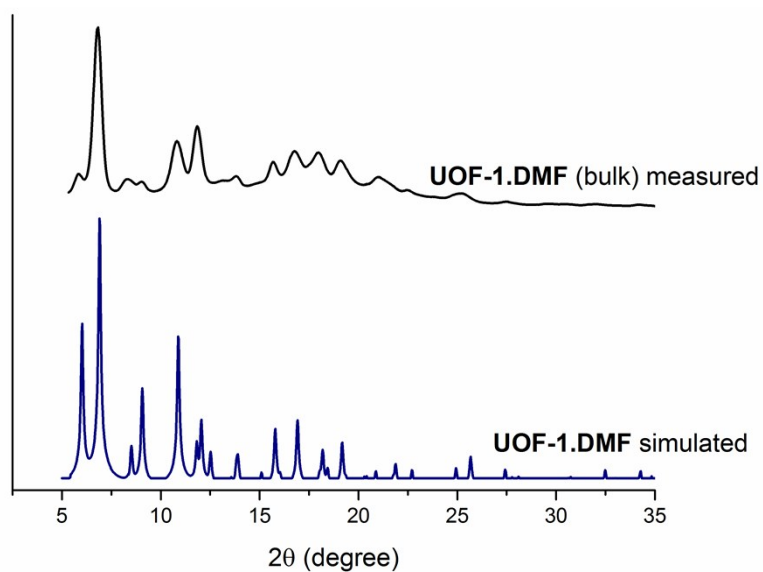


Figure S5. The simulated and the actual PXRD pattern of bulk sample of **UOF-1.DMF** showing phase purity of the material.

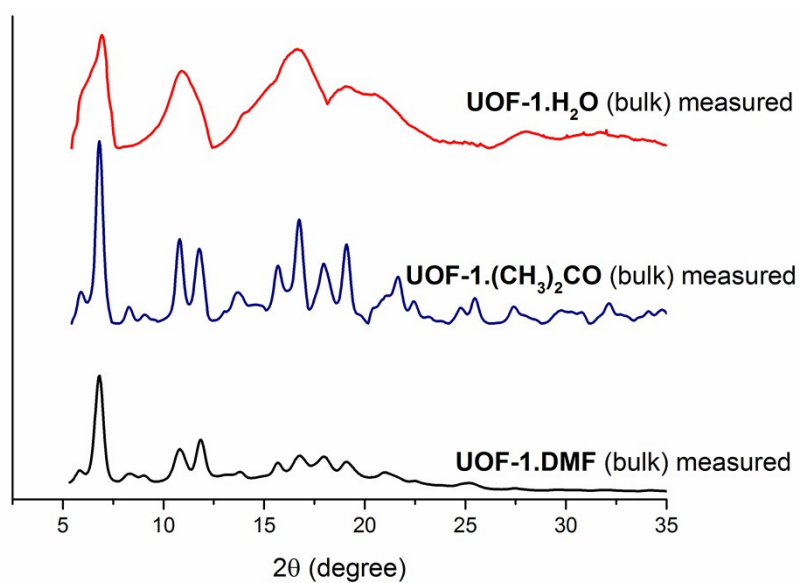


Figure S6. The actual PXRD pattern of bulk sample of **UOF-1.DMF**, **UOF-1.(CH₃)₂CO** and **UOF-1.H₂O** showing stability of the material in water.

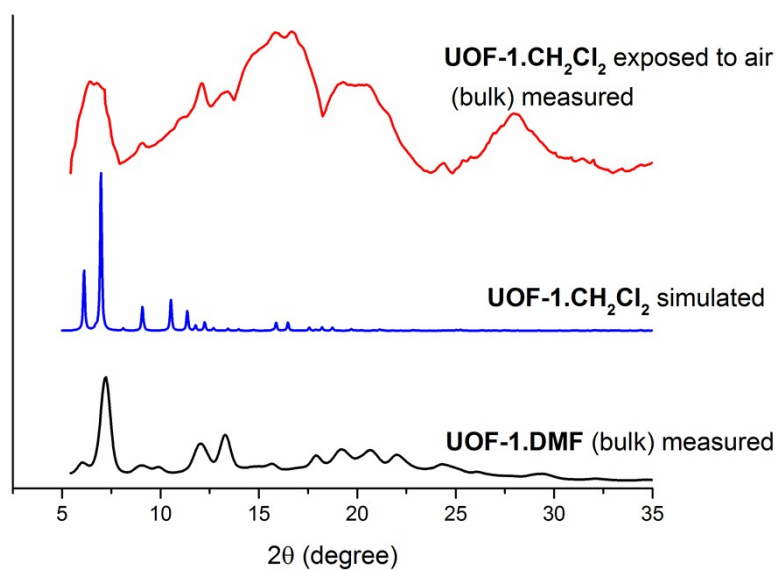


Figure S7. The simulated PXRD pattern of **UOF-1.CH₂Cl₂** and the actual pattern of bulk sample of **UOF-1.DMF** and **UOF-1.CH₂Cl₂** when exposed to air showing broadening of peaks due to the presence of moisture from the atmosphere.

S1.6 Activation Techniques

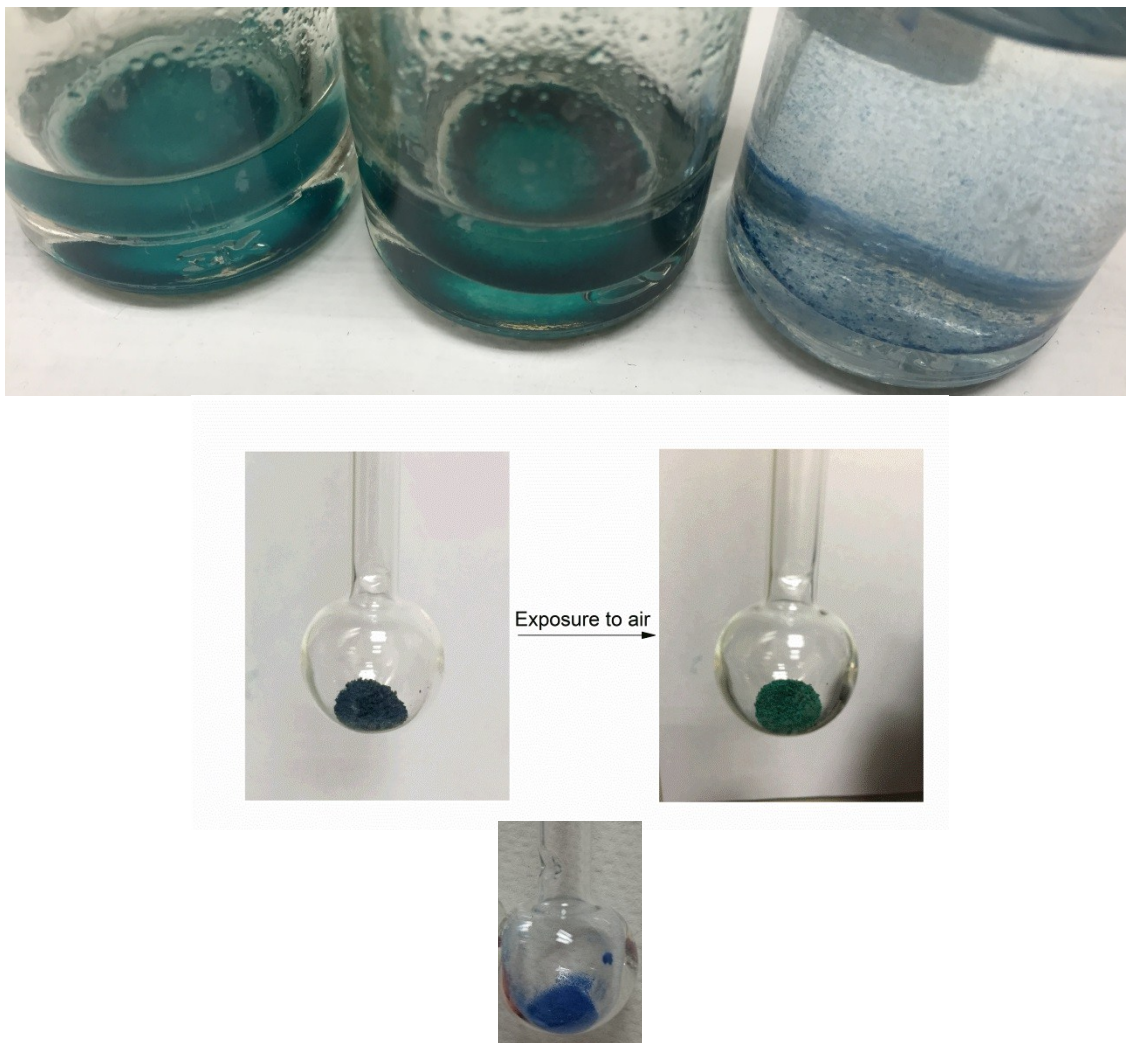


Figure S8. Top: The images of as-synthesized **UOF-1**·(CH_3) $_2$ **CO** (left), **UOF-1**·**DMF** (middle) and **UOF-1**· CH_2Cl_2 (right) showing the difference in colour upon soaking in CH_2Cl_2 . Middle: The images of the **UOF-1**· CH_2Cl_2 crystals which were dried under high vacuum for 14 hours (left) and the colour change observed in this sample upon exposure to air. Bottom: The image of the **UOF-1**· s-CO_2 obtained by activating **UOF-1**·**DMF** with supercritical CO_2 followed by exposure to a dynamic vacuum at 298 K.

S1.6.1 Procedure for activation of UOF-1E and UOF-1F

A freshly prepared **UOF-1.DMF** sample was obtained from a single synthesis batch and activated by soaking in dry CH_2Cl_2 . The DMF solvent from these crystals was removed and 10 mL of dry CH_2Cl_2 was added to it. After 10 minutes, the solvent was removed and replenished with fresh dry CH_2Cl_2 . This process was repeated 3-4 times and the crystals were then soaked in dry CH_2Cl_2 for 24 hours. After 24 hours, the solvent was removed and fresh dry CH_2Cl_2 solvent was added. This resulted in a change of the crystal colour from turquoise to dark blue after which these crystals were transferred to a pre-weighed analysis tube. The excess CH_2Cl_2 was removed under dynamic vacuum at 10^{-6} torr by heating the tube at 298 K for 40 hours. The sample mass was calculated using the degassed sample after the sample tube was backfilled with N_2 gas. The sample mass recorded was 29.7 mg.

Another sample was activated using supercritical CO_2 (**UOF-1.s- CO_2**). The solvent of the freshly prepared single crystals of **UOF-1.DMF** was exchanged with dry acetone over three days and the solvent was removed and fresh solvent was replenished each day. On the fourth day, the solvent was removed and then the crystals were activated with five purges with liquid CO_2 over three hours, conversion to the supercritical state and standing overnight, followed by a slow bleed of the CO_2 over several hours. The sample was then placed in a sample tube whilst minimising exposure to the atmosphere then subjected to a dynamic vacuum at 10^{-6} torr with heating to 298 K for 20 hours. This heating/vacuum step resulted in a change of the crystal colour from turquoise to dark blue. The sample mass was calculated using the degassed sample after the sample tube was backfilled with N_2 gas.

S1.7 Gas adsorption isotherms of UOF-1.CH₂Cl₂ and UOF-1.s-CO₂

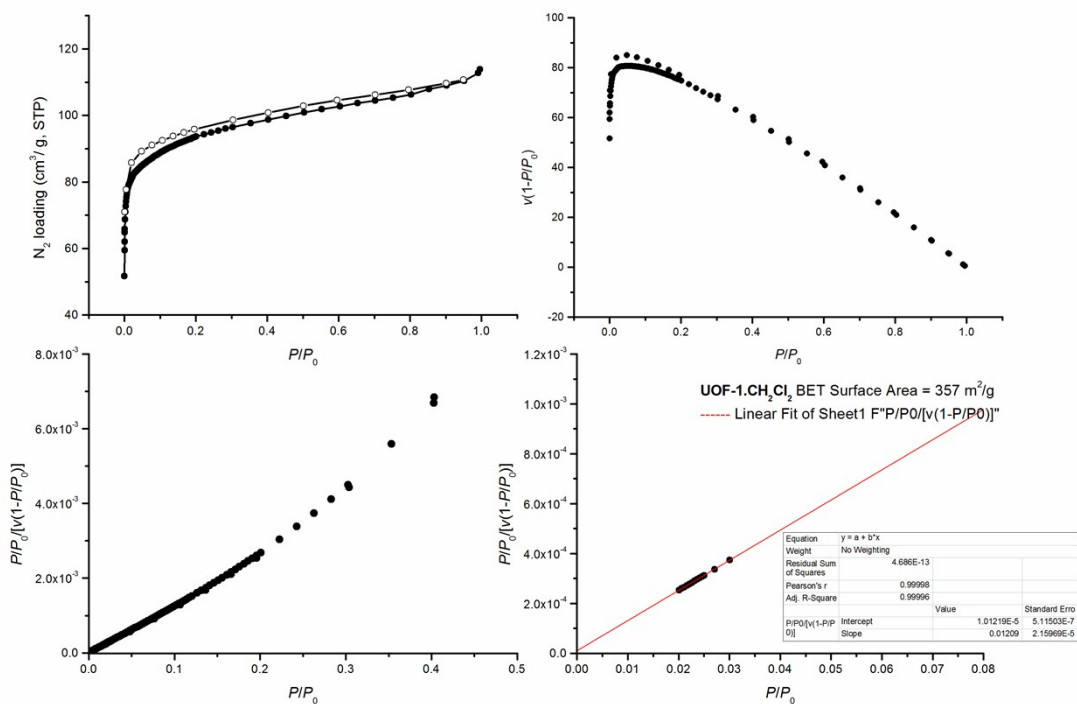


Figure S9. N₂ adsorption isotherm at 77 K with adsorption shown as filled markers and desorption shown as hollow markers together with BET surface area plots for activated UOF-1.CH₂Cl₂.

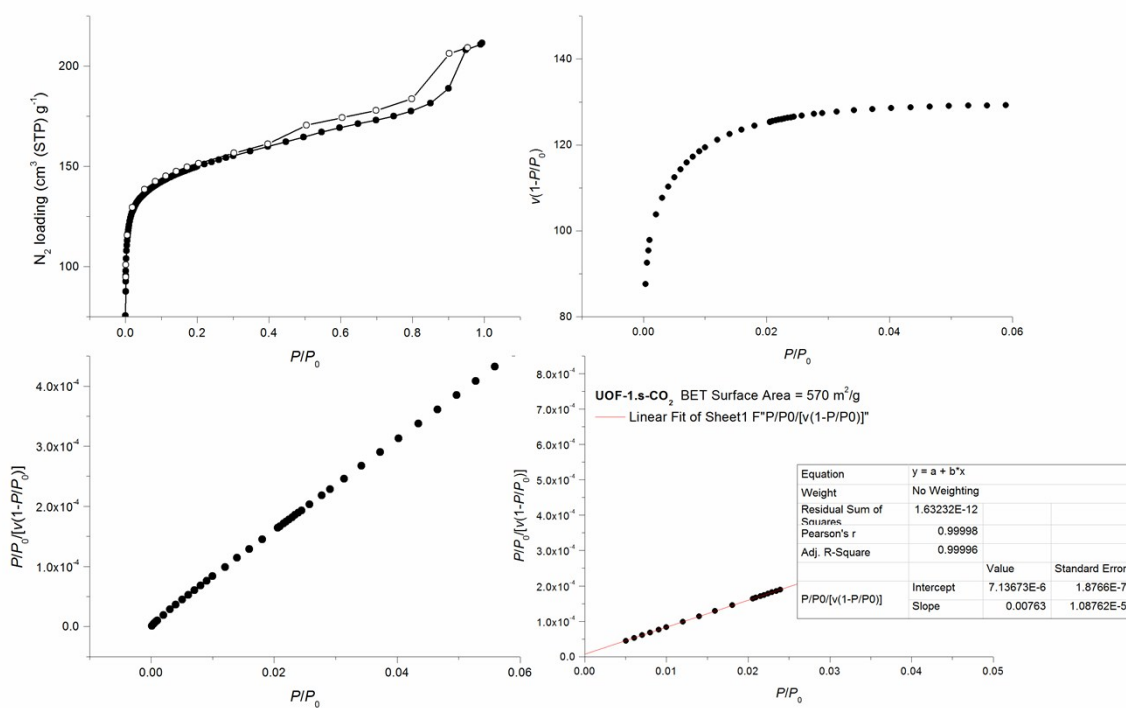


Figure S10. N₂ adsorption isotherm at 77 K with adsorption shown as filled markers and desorption shown as hollow markers together with BET surface area plots for activated UOF-1.s-CO₂.

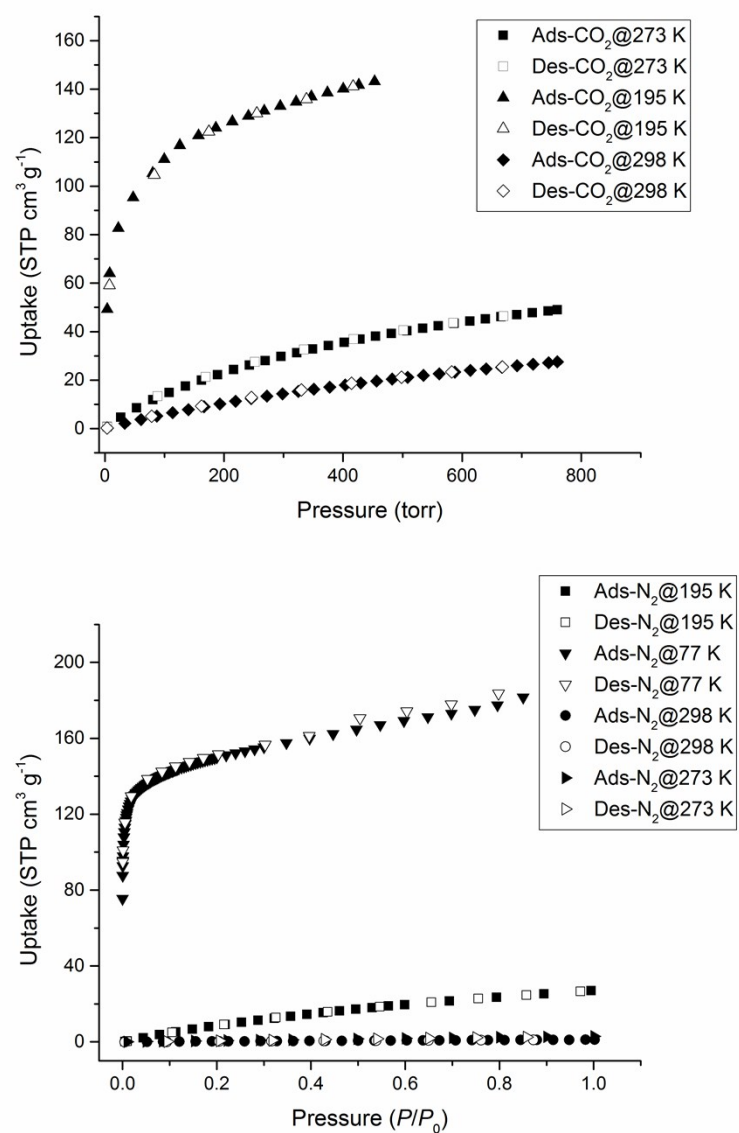


Figure S11. The plot of isotherms for UOF-1.s-CO₂ with adsorption shown as filled markers and desorption shown as hollow markers.

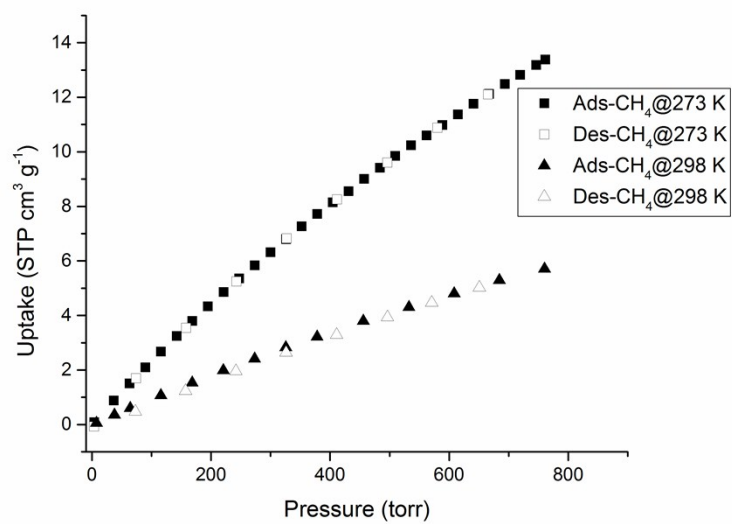
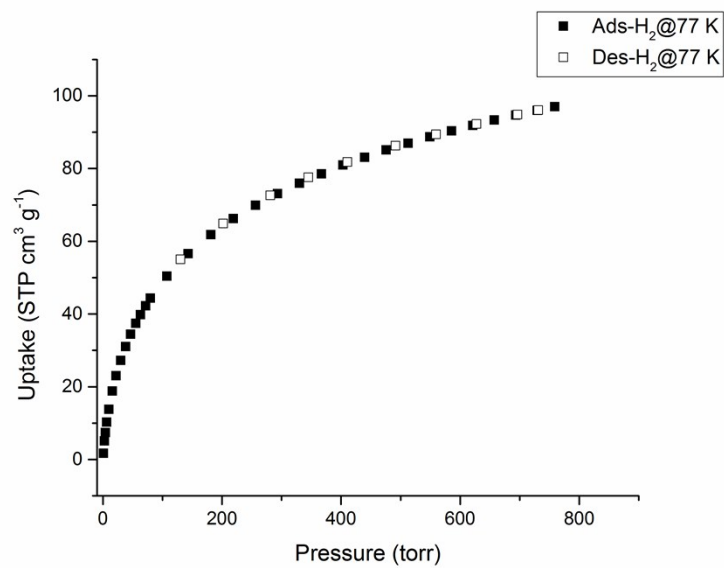


Figure S12. The plot of isotherms for UOF-1.s-CO₂ with adsorption shown as filled markers and desorption shown as hollow markers.

S1.7.1 Gas Adsorption Summary

Table S2. A summary of the UOF-1.CH₂Cl₂ and UOF-1.s-CO₂ gas adsorption results

| Gas | Temperature (K) | Amount adsorbed by UOF-1.s-CO ₂ at P = 1 bar (cm ³ g ⁻¹) | | | Amount adsorbed by UOF-1.CH ₂ Cl ₂ at P = 1 bar (cm ³ g ⁻¹) |
|-----------------|-----------------|--|----------------|----------------|--|
| | | Measurement 1 | Measurement 2 | Measurement 3 | |
| N ₂ | 77 | 212 | 227 | 213 | 114 |
| | 195 | 26.9 | 46.0 | 32.0 | 24.3 |
| | 273 | 2.89 | 16.8 | 4.50 | 3.32 |
| | 298 | 1.16 | Not measurable | Not measurable | Not measurable |
| CO ₂ | 195 | 143* | 177* | 140* | 109* |
| | 273 | 49.0 | 89.8 | 48.7 | 43.7 |
| | 298 | 27.5 | 43.1 | 30.2 | 27.9 |
| CH ₄ | 273 | 13.4 | 30.7 | 14.9 | 13.0 |
| | 298 | 5.71 | 8.62 | 5.54 | 6.19 |
| H ₂ | 77 | 97.0 | 158 | 119 | Not measured |

* gas adsorbed at 0.6 bar

S1.8 Comparative Data of Cu-PtS Structures in the Literature

Table S3. A summary of the literature review on Cu-PtS structures

| MOFs | Type of network | Type of activation | SA (m ² g ⁻¹) [#] | Pore Dimensions (Å) | Potential void volume (%) | Ref |
|--|------------------------|---|---|---------------------|---------------------------|-----------|
| {[Cu ₂ (H ₂ O) ₂ (A1)]·nDMF} _∞ | Non-interpenetrated | Thermal | 685 | 2.7×9.9, 5.1×8.3 | 58 | 4 |
| {[Cu ₂ (H ₂ O) ₂ (A1)]·4DMA·2H ₂ O} _∞ | Non-interpenetrated | (CH ₃) ₂ CO exchange + Vacuum drying | 382 | 2.7×9.9, 5.1×8.3 | 48 | 5 |
| {[Cu ₂ (A2)(H ₂ O) ₂]·6DEF·2H ₂ O} _∞ | Non-interpenetrated | CH ₂ Cl ₂ exchange + Vacuum drying | 526 | 19.5×7, 8.4×7 | 72 | 6 |
| | | CH ₂ Cl ₂ exchange + Freeze drying | 1560 | | | |
| {[Cu ₂ (A3)(H ₂ O) ₂]·14DEF·5H ₂ O} _∞ | 2-fold interpenetrated | CH ₂ Cl ₂ exchange + Vacuum drying | 791 | 21.2×3.5, 7.4×7.4 | 73 | 7 |
| | | CH ₂ Cl ₂ exchange + Freeze drying | 1020 | | | |
| {[Cu ₂ (A4)(DMF) ₂]·2DMF·4H ₂ O} _∞ | Homo-crossed network | CH ₂ Cl ₂ exchange + Freeze drying | 555 | 10×8.9 | 42 | 7 |
| {[Cu ₂ (A5)(H ₂ O) ₂]·12DEF·26H ₂ O} _∞ | 2-fold interpenetrated | CH ₂ Cl ₂ exchange + Freeze drying | 262 | 25.6×10.6 | 79 | 8 |
| MOF-11 | Non-interpenetrated | Thermal | 560 ^a | 6–6.5 | 50 | 8 |
| {[Cu ₂ (A6)(H ₂ O) ₂]·14DMF·10H ₂ O} _∞ | Non-interpenetrated | Not mentioned | 1217 ^a (calc. 6044) ^b | 10×10, 25×5 | 81 | 9 |
| {[Cu ₂ (A7)(H ₂ O) ₂]·13DMF} _∞ | Non-interpenetrated | (CH ₃) ₂ CO exchange + Vacuum drying | 733 ^a | 9×9 | 75 | 10 |
| UOF-1 | Non-interpenetrated | CH ₂ Cl ₂ exchange + Vacuum drying | 357 | 26.1×12, 14.7×9.7 | 79 | This work |
| | | (CH ₃) ₂ CO and s-CO ₂ exchange + Vacuum drying | 570 | | | |

H₄A1 = tetrakis[4-(carboxyphenyl)oxamethyl]methane; H₄A2 = tetrakis(4-carboxyphenyl)methane; H₄A3 = tetrakis(4-carboxyphenyl-4-phenyl)methane; H₄A4 = tetrakis(4-carboxyphenylethene)methane; H₄A5 = tetrakis(4-carboxyphenylethynyl-4-phenyl)methane; H₄A6 = 5',5''-(4-carboxyphenyl)-2',6''-dihydroxy-[1,1':3',1''':3'',1''''-Quaterphenyl]-4,4'''-dicarboxylic acid ; H₄A7 = 5',5''-(4-carboxyphenyl)-2',6''-diethoxy-[1,1':3',1''':3'',1''''-Quaterphenyl]-4,4'''-dicarboxylic acid

[#]Surface area measured by BET isotherm unless specified as (a) Langmuir surface area (b) calculated surface area using GCMC simulations

S1.9 Pore Size Distribution

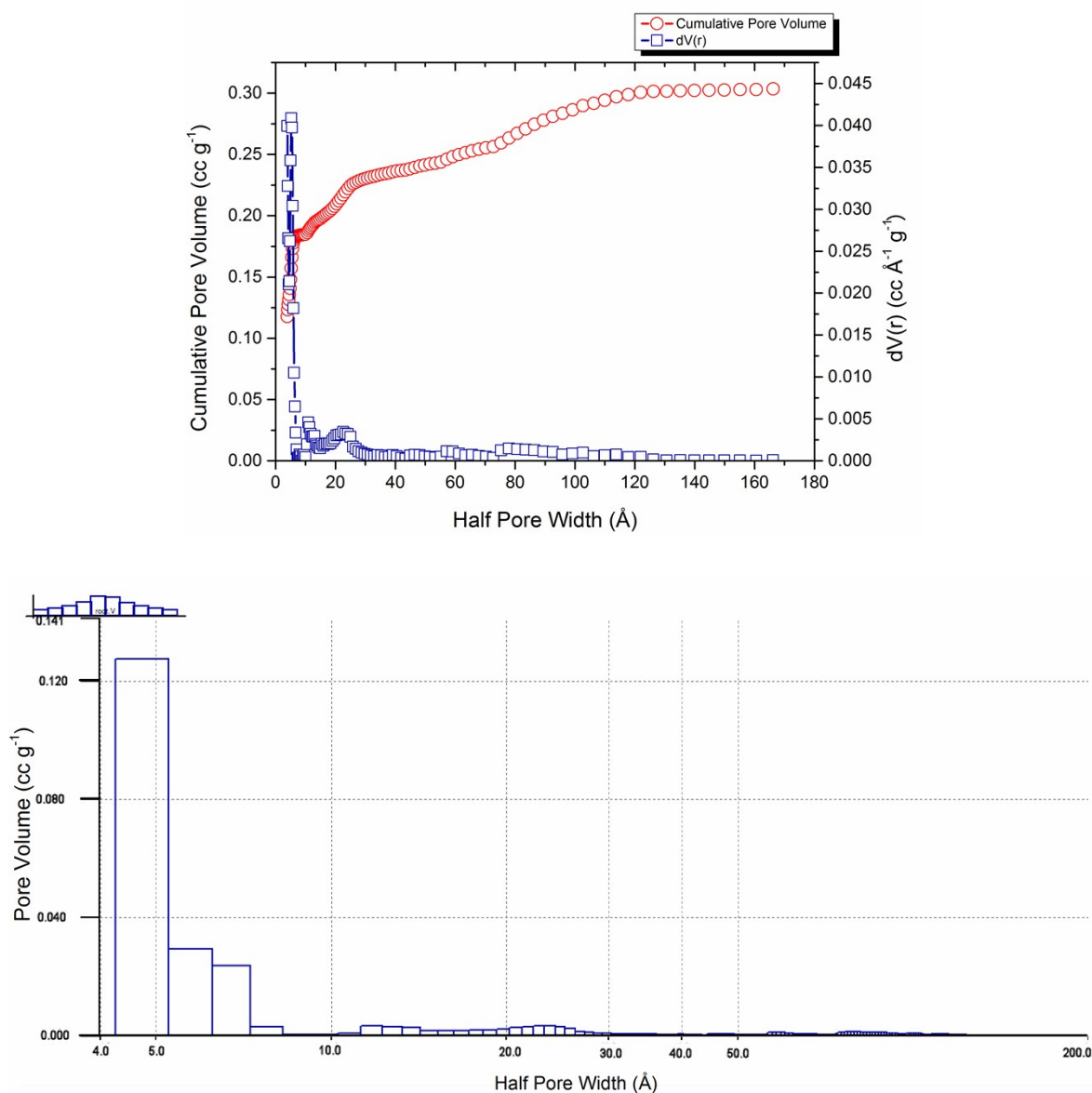


Figure S13. The pore size distributions calculated using the QSDFT method from the N₂ isotherm of UOF-1.s-CO₂ at 77 K using a slit-cylindrical adsorption kernel.

Table S4. A summary of the QSDFT method

| | |
|------------------------|--|
| Pore Volume | 0.303 cc g ⁻¹ |
| Surface area | 607.579 m ² g ⁻¹ |
| Lower confidence limit | 3.925 Å |
| Fitting error | 0.065% |
| Half pore width (Mode) | 5.255 Å |
| Moving point average | Off |

S1.10 Ideal Adsorbed Solution Theory (IAST) Calculations

Dual-site Langmuir (DSL) was found to be the best model for fitting each gas adsorption isotherms at 273 K. DSL is the sum of Langmuir isotherm models for two types of sites and is expressed as:

$$N(P) = M_1 \frac{K_1 P}{1 + K_1 P} + M_2 \frac{K_2 P}{1 + K_2 P}$$

where M_i is the number of adsorption sites of type i , which have Langmuir constant K_i .

The selectivity for a mixture of 15% CO₂ and 85% CH₄ or N₂ at 273 K was calculated based on the IAST method using pyIAST¹¹

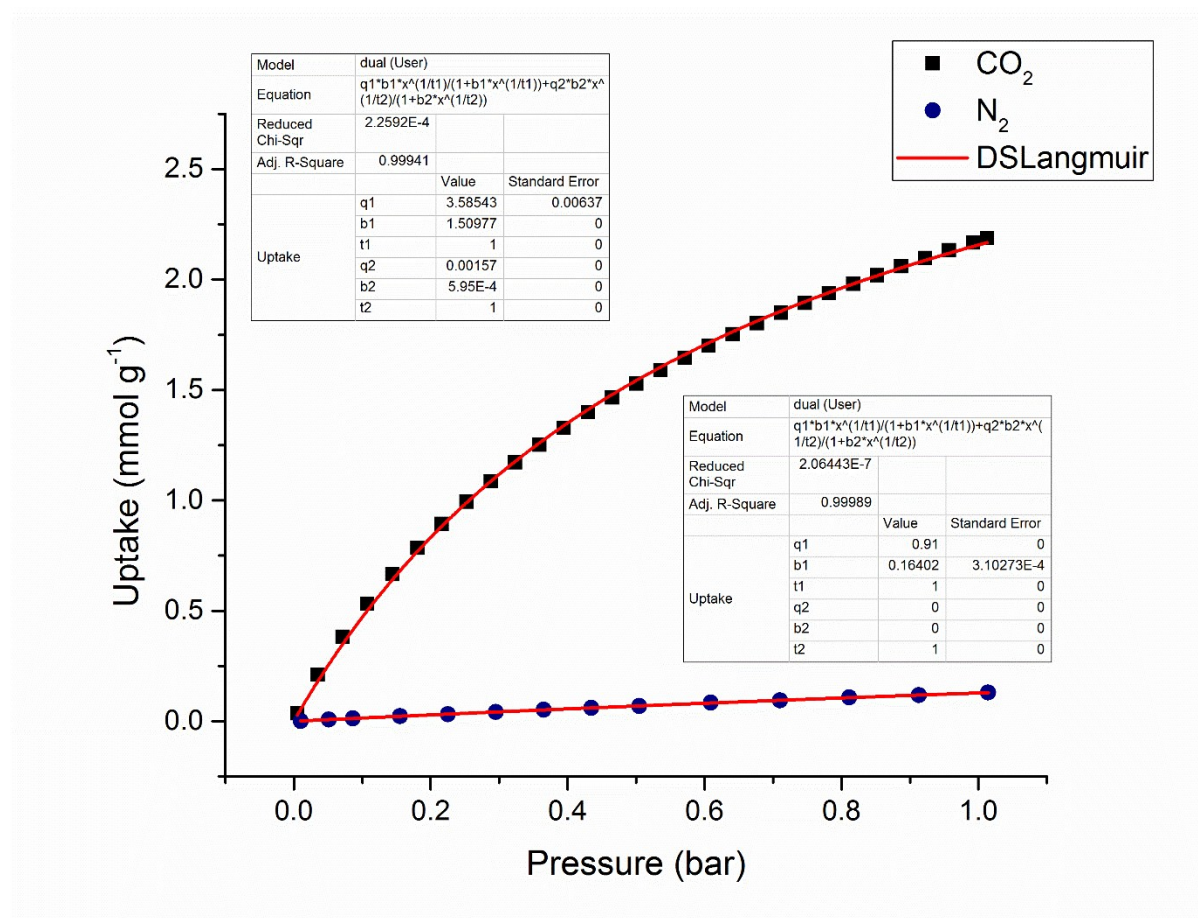


Figure S14. Isotherm fitting parameters for UOF-1.s-CO₂ at 273 K.

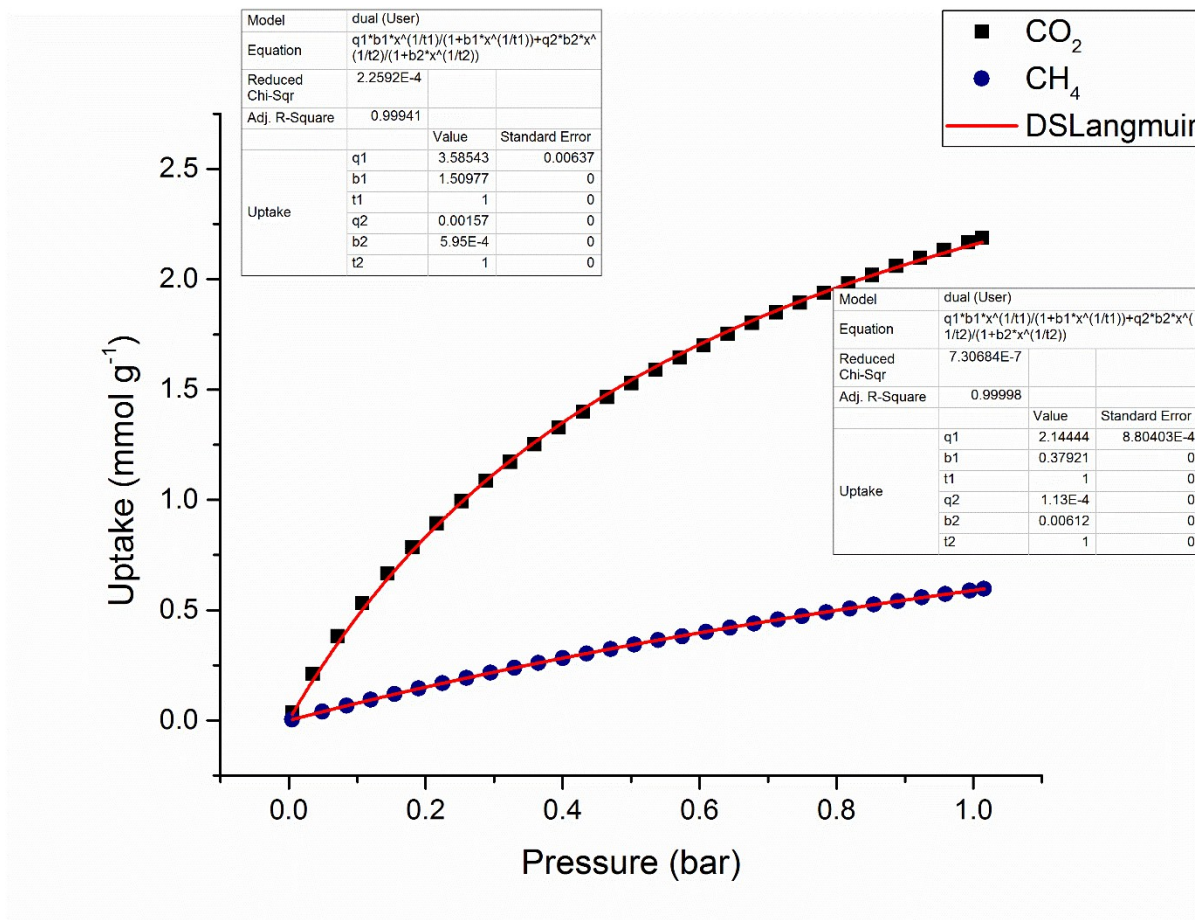


Figure S15. Isotherm fitting parameters for UOF-1.s-CO₂ at 273 K.

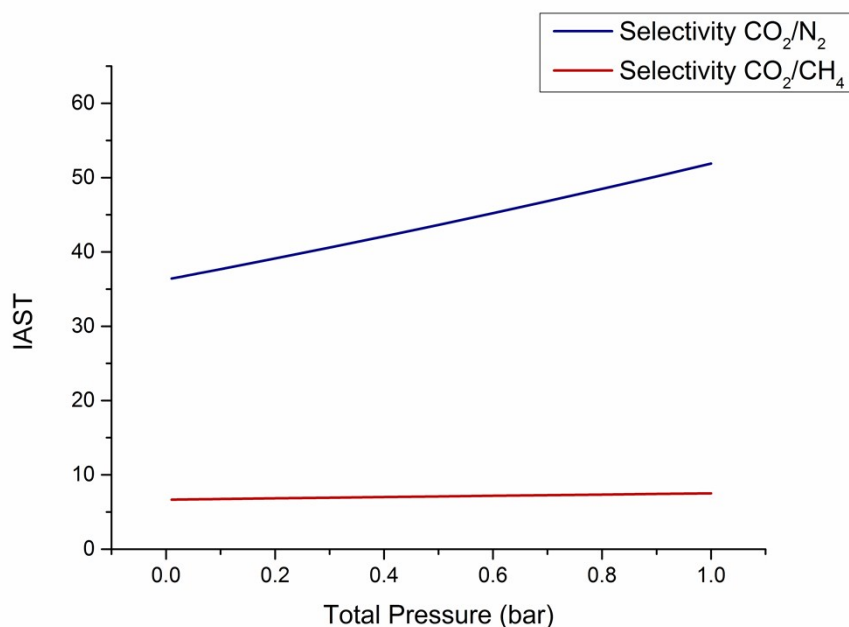


Figure S16. The selectivity for a mixture of 15% CO₂ and 85% N₂ (in blue) and 15% CO₂ and 85% CH₄ (in red) at 273 K was calculated based on the IAST method using pyIAST.

S1.11 Heat of Adsorption (Q_{st}) Calculations

The isosteric heat of adsorption (Q_{st}) values were calculated from CO_2 and CH_4 isotherms measured at 273 K and 298 K. These isotherms were first fitted to a virial equation given below:

$$\ln P = \ln N + \frac{1}{T} \sum_{i=0}^m a_i N^i + \frac{1}{T} \sum_{i=0}^n b_i N^i$$

The fitting parameters from the above equation were used as follows to calculate Q_{st} :

$$Q_{st} = -R \sum_{i=0}^m a_i N^i$$

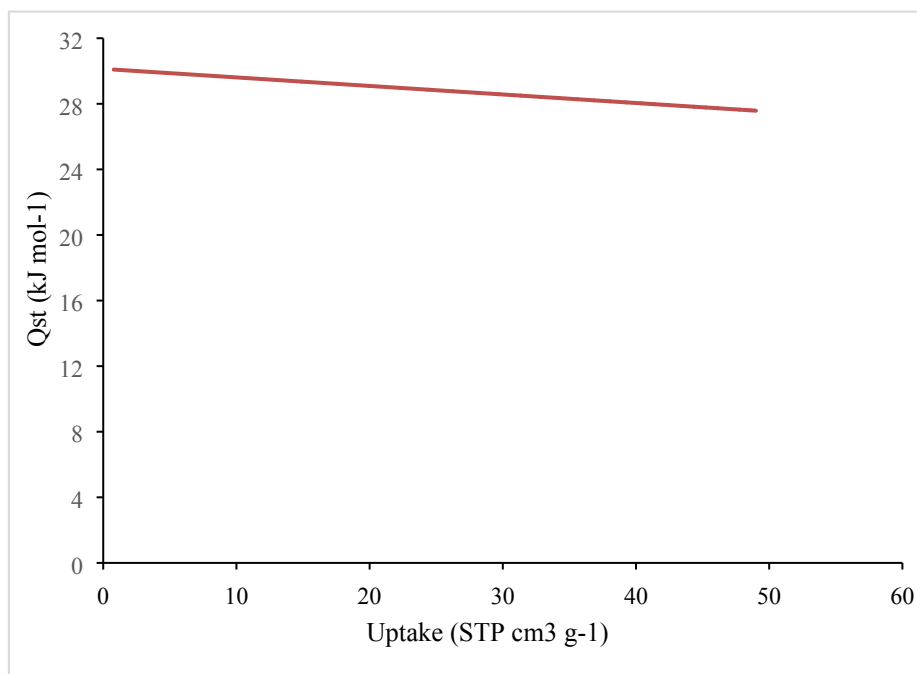
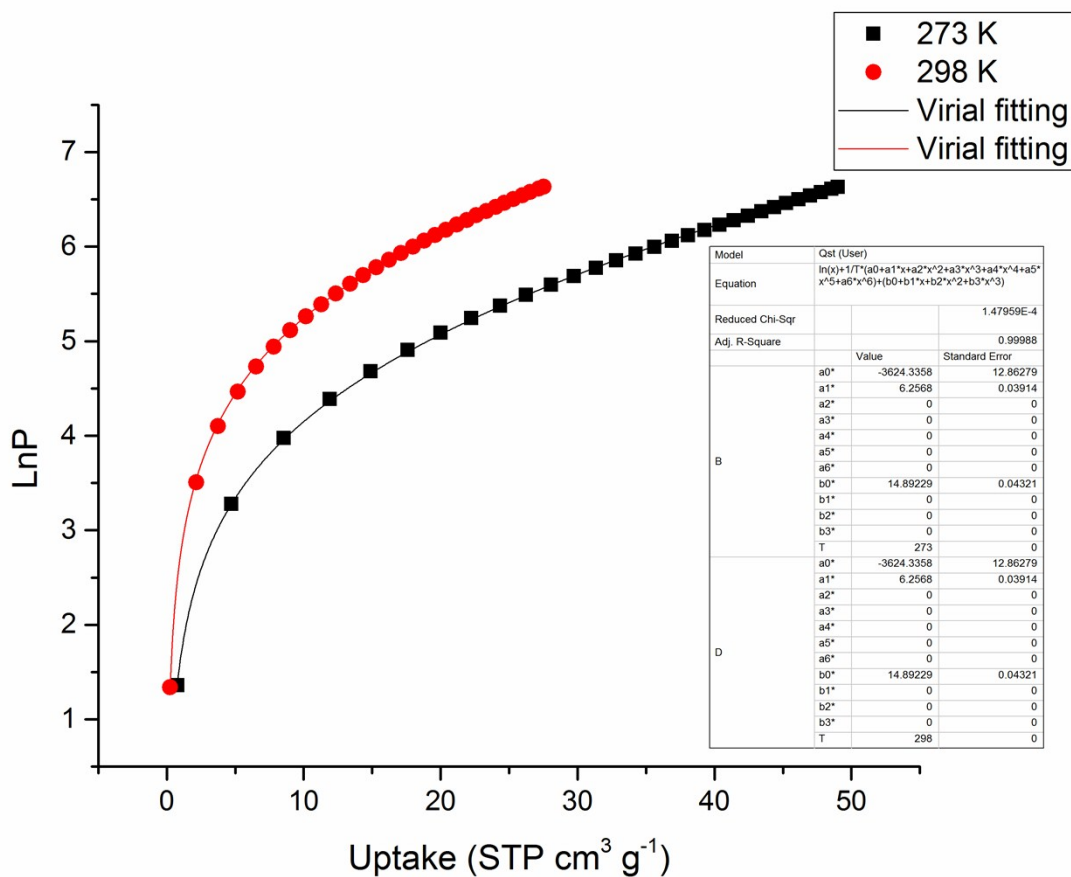


Figure S17. Top: Virial equation fit for CO₂ adsorption isotherms. Bottom: Isosteric heat of adsorption plot for the adsorption of CO₂ by UOF-1.s-CO₂.

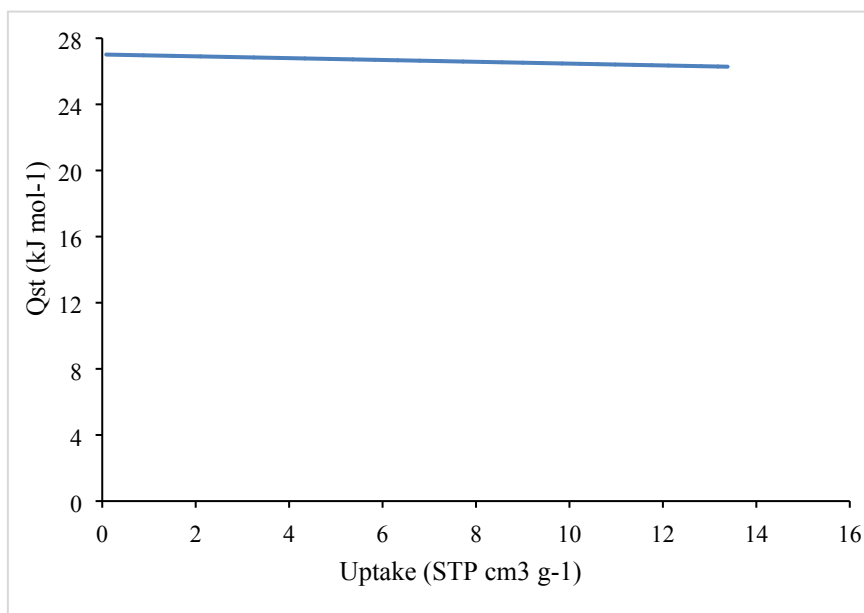
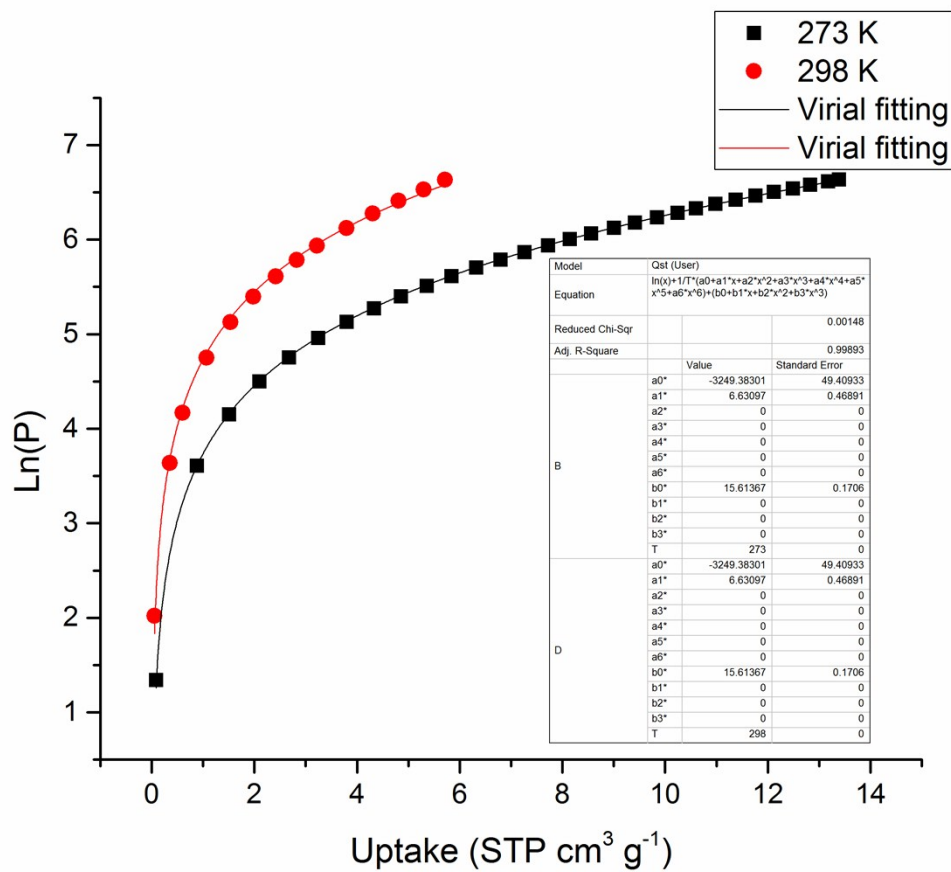


Figure S18. Top: Virial equation fit for CH₄ adsorption isotherms. Bottom: Isosteric heat of adsorption plot for the adsorption of CH₄ by UOF-1.s-CO₂.

S1.12 References

1. M. V. Marinho, M. I. Yoshida, K. J. Guedes, K. Krambrock, A. J. Bortoluzzi, M. Hörner, F. C. Machado and W. M. Teles, *Inorg. Chem.*, 2004, **43**, 1539-1544.
2. L. F. Marques, M. V. Marinho, C. C. Correa, N. L. Speziali, R. Diniz and F. C. Machado, *Inorg. Chim. Acta*, 2011, **368**, 242-246.
3. A. Spek, *Acta Crystallogr., C*, 2015, **71**, 9-18.
4. J. Tian, R. K. Motkuri and P. K. Thallapally, *Cryst. Growth Des.*, 2010, **10**, 3843-3846.
5. L.-L. Liang, J. Zhang, S.-B. Ren, G.-W. Ge, Y.-Z. Li, H.-B. Du and X.-Z. You, *CrystEngComm*, 2010, **12**, 2008-2010.
6. L. Ma, A. Jin, Z. Xie and W. Lin, *Angew. Chem., Int. Ed.*, 2009, **48**, 9905-9908.
7. D. Liu, Z. Xie, L. Ma and W. Lin, *Inorg. Chem.*, 2010, **49**, 9107-9109.
8. B. Chen, M. Eddaoudi, T. M. Reineke, J. W. Kampf, M. O'Keeffe and O. M. Yaghi, *J. Am. Chem. Soc.*, 2000, **122**, 11559-11560.
9. S. Wu, L. Ma, L.-S. Long, L.-S. Zheng and W. Lin, *Inorg. Chem.*, 2009, **48**, 2436-2442.
10. L. Ma, J. Y. Lee, J. Li and W. Lin, *Inorg. Chem.*, 2008, **47**, 3955-3957.
11. C. M. Simon, B. Smit and M. Haranczyk, *Comput. Phys. Commun.*, 2016, **200**, 364-380.